



## Original article

## Voltage dependent pulse shape analysis of Geiger-Müller counter

B. Almutairi<sup>a, c</sup>, T. Akyurek<sup>b</sup>, S. Usman<sup>a, \*</sup><sup>a</sup> Department of Mining and Nuclear Engineering, Missouri University of Science & Technology, Rolla, MO, 65401, USA<sup>b</sup> Department of Physics, Faculty of Art and Science, Marmara University, 34722, Kadikoy, Istanbul, Turkey<sup>c</sup> Environmental and Life Sciences Center, Kuwait Institute for Scientific Research, Kuwait City, 13109, Kuwait

## ARTICLE INFO

## Article history:

Received 30 July 2018

Received in revised form

2 February 2019

Accepted 10 February 2019

Available online 13 February 2019

## ABSTRACT

Detailed pulse shape analysis of a Geiger-Müller counter is performed to understand the pulse shape dependence on operating voltage. New data is presented to demonstrate that not all pulses generated in a GM counter are identical. In fact, there is a strong correlation between the operating voltage and the pulse shape. Similar to detector deadtime, pulse shapes fall in three distinct regions. For low voltage region, where deadtime was reported to reduce with increasing voltage, pulse generated in this region was observed to have a fixed pulse width with a variable tail. The pulse width and fall time of the tail was observed to be a function of applied voltage; exponentially reducing with increasing voltage with an exponent of negative 6E-04 and 2E-03 respectively. The second region showed a pulse without any significant tail. During this time the detector deadtime was earlier reported to be at its minimum. The highest voltage region demonstrated a different deadtime mechanism where the second pulse was reduced in width. During this time the deadtime seemed to be increasing with increasing voltage. This data allows us to gain some unique insight into the phenomenon of GM detector deadtime not reported thus far.

© 2019 Korean Nuclear Society, Published by Elsevier Korea LLC. This is an open access article under the CC BY-NC-ND license (<http://creativecommons.org/licenses/by-nc-nd/4.0/>).

## 1. Introduction

Geiger-Mueller (GM) counter is one of the oldest radiation detectors which was introduced by Geiger and Müller in 1928 [1]. It is widely used in the measurement of radiation due to its inexpensive, simple, rugged design and ease of operation. The GM counter falls under the category of filled gas detectors. It operates on the principle of gas multiplication, i.e., electron and positive ion pairs are created from an initial radiation interaction. Due to the high velocity of charged particles, secondary ionization events are produced. If the original ionizing event was caused by beta or alpha particles, then the fill gas is ionized directly; on the other hand, gamma and x-rays ionize the gas indirectly.

When a high voltage is applied to the detector, the electrons are accelerated towards the anode and the positive ions are accelerated towards the cathode due to the potential difference between the anode and cathode. The accelerated electron gains sufficient kinetic energy to produce secondary ionization. In addition to the secondary ionization a large number of atoms/molecules are left in the

excited state leading to almost immediate de-excitation of these molecules which produce photons within visible or ultraviolet range. Interaction of these photons with the GM cathode wall or the gas itself causes secondary and tertiary ionizations, eventually leads to the formation of an avalanche of ion pairs commonly known as Townsend avalanche [2]. Under proper conditions, an avalanche can trigger a second avalanche, however, at a different position within the counter. On the average, each avalanche can trigger at least another avalanche; thus, a self-propagating chain reaction that envelopes the entire anode's wire is induced. The velocity at which the avalanche propagates is approximately 2–4 cm/μs [2]. At higher values of the electric field, within a very short time an exponentially growing number of avalanches are formed. At certain point when the avalanche has reached the maximum size, the chain reaction terminates. Because of that, all pulses produced by the GM counter are generally believed to be of the same amplitude and shape. The GM counter is therefore limited in its application and cannot be used for radiation spectroscopy [2]. Data presented here makes this general assumption that all GM pulses are identical questionable.

Furthermore, the collected negative charges that were produced in the detector results in a pulse that lasts for a few microseconds. The time it takes to collect the charge depends on various factors:

\* Corresponding author. Missouri University of Science & Technology, Rolla, MO, USA.

E-mail address: [usmans@mst.edu](mailto:usmans@mst.edu) (S. Usman).

temperature, pressure, type of gas in the detector and the applied voltage; whereas the duration of the pulse depends on other factors: detector geometry, initial ionization location within the detector and the applied voltage [3]. The speed at which electrons or positive ions move from their point of origin can be accurately predicted by;

$$v = \frac{\mu \cdot \varepsilon}{p} \quad (1)$$

where  $v$  is the drift velocity,  $\mu$  is the charge mobility,  $\varepsilon$  is the strength of the electric field and  $p$  is the gas pressure. The mobility of free electrons in gases is much larger than that of positive ions; however, at higher electric field values, positive ion's drift velocity increases slowly with the electric field until it reaches a saturation velocity. Any further increase in the electric field will not affect the mobility, it will remain constant over a wide ranges of electric field and gas pressure for both the negative electron and the positive ions. Typical mobility for gases with a medium atomic number falls in the range of  $1\text{--}1.5 \times 10^{-4} \text{ m}^2 \text{ atm/V. sec.}$  and a typical drift velocity of 1 m/s occurs at 1 atm pressure and an electric field of  $10^4 \text{ V/m}$  as reported in the literature [2].

Nevertheless, free electrons and positive ions behave differently under applied voltage in that the former is more mobile than the latter by a factor of 1000 due to their low masses. Therefore, the collection time of free electrons is in the order of microseconds whereas the collection time of ions is in the order of milliseconds [3]. May et al. [4] proposed that the drift velocity of ions is inversely proportional to temperature. Other studies have confirmed that ion mobility is not only altered by the applied voltage but also by temperature [3]. Preliminary work on temperature dependence of GM counter performance was reported by Akyurek and co-workers [3] and will not be discussed here.

Unlike free electrons which are collected rapidly at the anode, positive ions take a longer time to be collected at the cathode due to their low mobility. Under proper conditions, the positive ions form a sheath around the anode which results in a distortion of the electric field. If the sheath space of positive ions around the anode is not completely removed, any subsequent pulse generated will be reduced in amplitude. If the distorted field lingers and becomes stronger in magnitude, any following radiation interaction within the counter may result in an undetectable pulse [3,5]. This undetectable pulse is lost in the GM counter. Since radiations incidents are random in nature, it follows that many undetectable pulses are lost in the counter. The undetectable pulses are a consequence of a phenomenon called *deadtime* which is yet another limitation of the GM counters.

### 1.1. The deadtime problem

Deadtime is defined as the minimum time interval required for two consecutive radiation interactions in the counter to be detected as independent events. When two events occur within a short duration of time, less than the minimum time interval, the detector is unresponsive (dead); hence, the event is lost [6]. Detector deadtime had been an active area of research, several theoretical and experimental studies in the 30s and 40s have shown that the GM counter suffers from a long deadtime in the order of a few hundred microseconds to several milliseconds [7,8]. For low counting rate applications, the GM counter has been extensively used where counting loss is rather easy to correct. On the other hand, for high counting rate applications, scintillation or solid-state detectors are better suited to perform the task because they suffer from a shorter deadtime [9]. It is for this reason that correction of deadtime of GM counters for high counting rate applications has been largely neglected until the late 1990s where the problem was reinvestigated by a group of researchers [10,11]. In general, for various radiation detectors, deadtime phenomenon is significant at high intensity radiation applications such as in Positron Emission Tomography (PET) and spent fuel scanning. For gas-filled detectors, the investigation further continued to extend the useful counting rate range of GM counters [9,12,13].

It is important to recognize that deadtime is added at all stages of signal processing. As can be seen in Fig. 1, radiation detection system consists of a detector that produces the initial pulse and passes it to a series of electronic pulse processing instruments; preamplifier, amplifier, single channel analyzer (SCA), and then either a multichannel channel analyzer (MCA) or a counter records the pulse [14]. In a typical radiation detection system, there are two elements that contribute to total deadtime. First, the inherent deadtime produced by the detector's physical process and electric circuitry. Second, the characteristic deadtime contributed by each electronic instrument in the system. The deadtime from the modern electronics is negligible as compared to the long deadtime that GM detectors suffer from Refs. [14,15]. Therefore, pulse processing deadtime can be neglected and only the inherent deadtime of the detector is sufficient for count rate correction consideration.

### 1.2. Detector deadtime models

There are two widely used models for deadtime behavior in counting systems: the paralyzing model also known as the extending type; and the non-paralyzing model also refer to as non-extending type. These are ideal models and were first proposed by Feller [16] and Evans [17]. The paralyzing model assumes that after

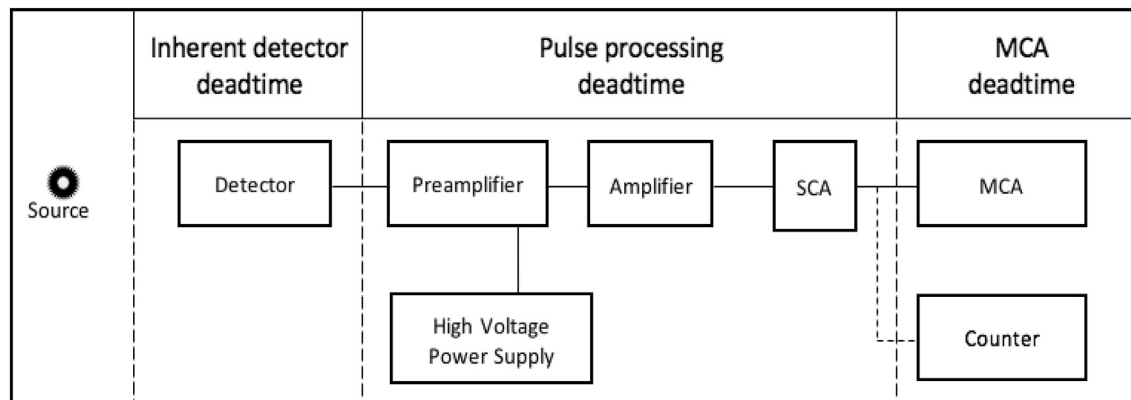


Fig. 1. Radiation detection system in a laboratory.

the first pulse is generated, any radiation incident that occurs during the resolving time (deadtime) will result in losing the subsequent pulse and it will reset the deadtime time; thus, the deadtime is extended. The system, therefore, suffers from continuous paralysis until at least a duration equal to or greater than the deadtime lapses without the occurrence of any radiation event. The mathematical description derived by Feller and Evans for the paralyzing model is given by;

$$m = n.e^{-n.\tau} \quad (2)$$

Where,  $m$  is the observed or measured count rate,  $n$  is the true count rate and  $\tau$  is the detector deadtime. The paralyzing model therefore sets the lower limit of deadtime behavior in a counting systems. For the non-paralyzing model, any radiation event that occurs during the deadtime will be lost but the deadtime does not extend. In this model, the detector is assumed to be dead for a fixed time  $\tau$  following each recorded radiation event. The mathematical description for the relation between observed and true counts for the non-paralyzing model is given by;

$$m = \frac{n}{1 + n.\tau} \quad (3)$$

where definitions of  $m$ ,  $n$  and  $\tau$  are the same as in Eq. (2). The non-paralyzing model therefore sets the upper limit of deadtime behavior for a counting systems. These ideal models have been used extensively with success; however, in a limited fashion. In reality, true deadtime characteristics fall somewhere in between these extreme limits because real detectors do not follow these ideal models [6,11,14].

In 2000, Lee and Gardner [11] in an effort to extend the counting range of the GM detector proposed a hybrid model that combines both ideal models into one analytical expression. Mathematically, the hybrid model is given by;

$$m = \frac{n.e^{-n.\tau_p}}{1 + n.\tau_{np}} \quad (4)$$

where  $\tau_p$  is the paralyzing deadtime and  $\tau_{np}$  is the non-paralyzing deadtime. In this hybrid model, Lee and Gardner assumed that the non-paralyzing deadtime depends on the physical characteristics of the detector itself. Based on this assumption, they proposed that paralyzing deadtime follows the non-paralyzing deadtime until a recorded amplitude is produced. However, they did not provide any justification for their assumption. In an effort to better represent the deadtime phenomenon, another hybrid model was proposed by Patil and Usman [12]. It was based on single deadtime and a fixed paralysis factor  $f$ , mathematically;

$$m = \frac{n.e^{-n.\tau.f}}{1 + n.\tau.(1-f)} \quad (5)$$

where  $\tau$  is the total deadtime and  $f$  is the paralysis factor. This fixed  $f$  is based on a probability that lies between 0 and 1. If the  $f$  is 1, then the hybrid model reduces to the ideal paralyzing model, while if  $f$  is 0, then the hybrid model reduces to the ideal non-paralyzing model. The hybrid models have successfully extended the useful counting range of the GM detector but only in a limited fashion. None of the models mentioned above have a phenomenological explanation of the deadtime; they are a mere mathematical convenience.

Recently, Usman and co-workers [18] demonstrated dependence of Geiger-Müller counter's deadtime on operating conditions. The their phenomenological model is based on a large

amount of data on deadtime and pulse shape properties for GM counter at varying operating voltages reported by Akyurek et al. [3]. The data demonstrate three different regions of detector deadtime with varying operating voltages, as shown in Fig. (2). In the low voltage deadtime region, the pulse width and tail duration were monotonically decreasing with increasing voltage. The occurrence of long exponentially decaying tail at the end of the pulse is believed to be due to the existence of some stray charge carriers in areas of weak potential. Those stray charge carriers take a longer time to be fully collected by the cathode due to the existence of space charge. If another radiation event takes place during this period, it will be lost; however, the system may or may not get paralyzed. Hence, paralysis depends on physical location of the second radiation event within the counter in relation to the stray charge. Since the exact location of the second radiation event within the counter is a random process and cannot be determined, a stochastic approach would be needed. It was therefore concluded that the paralysis factor, should be an exponentially decreasing function of the applied voltage between the time of onset of the tail and the occurrence of the second event, unlike the fixed value proposed by Patil and Usman [12].

In the plateau deadtime region (middle region), it was observed that there is a fixed deadtime independent of the applied voltage; hence, the GM counter behaves as a non-paralyzing detector and Eq. (3) can be used for that entire region. In the high voltage deadtime region, the occurrence of high concentrations of positive ions around the anode results in reduced electric field further which results in a weak second pulse. Because of the presence of higher space charge at higher voltages, longer deadtime durations were observed as experimental data from Akyurek et al. [3] confirmed. Therefore, GM counter in this region behaves as a non-paralyzing detector with deadtime monotonically increasing with increasing voltage. It reinforces the assumption that the GM counter is non-paralyzing in nature as previous studies have suggested [3,11,12].

Akyurek et al. [3] have shown that GM's deadtime phenomenon is dependent not only on applied voltages but also on operating temperatures and fatigues which ultimately result in alteration of the pulse shape properties. It is therefore concluded that a single deadtime model is not adequate for any detector under all operating conditions, and a careful selection of deadtime model under certain operating conditions is essential for the correction of observed count rates.

Current study present additional data on GM-counter deadtime and pulse shape for a wide range of operating voltage using  $^{60}\text{Co}$  and  $^{137}\text{Cs}$  sources. Raw data are provided and the analysis of result is shared with discussion on the variation of deadtime with operating voltage and pulse shape.

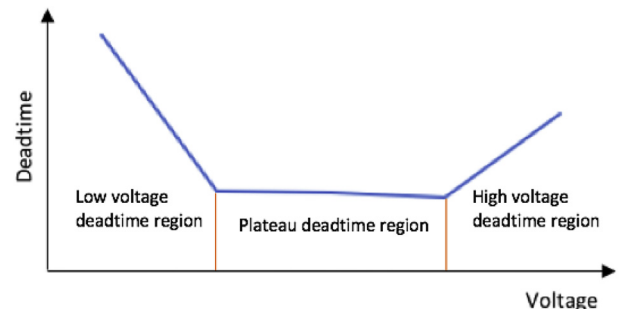


Fig. 2. Detector deadtime regions with voltage dependence.

2. Materials and method

The experimental set-up included: two sources, GM counter, preamplifier, high-voltage power supply, and an oscilloscope. <sup>60</sup>Co and <sup>137</sup>Cs were both used separately. Both sources were produced in February 2013 as 1 μCi strength and distributed by Spectrum Techniques, LLC [19].

The GM counter (Ludlum, model 133-2) was used for detecting radiation incidents [20]. Ludlum GM is a halogen quenched, stainless steel, windowless type detector which is more sensitive to gamma and x-ray radiations; alpha and beta particles are mostly blocked by the detector's thick walls. The typical deadtime value of this detector is reported by the manufacturer to falls in 50 μs range. A charge-sensitive preamplifier (Ortec, model 142A) was connected to the connector series “C” of the GM counter through a coaxial cable. The preamplifier's main function is to extract signals from the detector without degrading the intrinsic signal-to-noise ratio;

therefore, caution was exercised to ensure extracting low signal-to-noise ratio by placing the preamplifier as close to the detector as possible [21]. For high-voltage power supply, Ortec, model 556 was used and connected to the bias input of the preamplifier through a coaxial cable [22]. The Ortec 556 model was housed in a nuclear instrumentation module (NIM) and it provides noise-free, very stable high voltage necessary for proper operation of the GM counter. The input voltage can be controlled from an adjustable ±10 to ±3000 V knob. The input power is connected directly from the AC line. Finally, Oscilloscope (Tektronix, model DPO3032) was connected to the output of the preamplifier through a coaxial cable [23]. The oscilloscope was connected to the PC through a USB cable and the oscilloscope's screen image of pulses was saved directly to the PC. The DPO3032 has an automatic measurements mode which was utilized to acquire and record train of pulses. The automatic measurements mode is divided into two categories: time and amplitude measurements. Table (1) lists the illustration of various

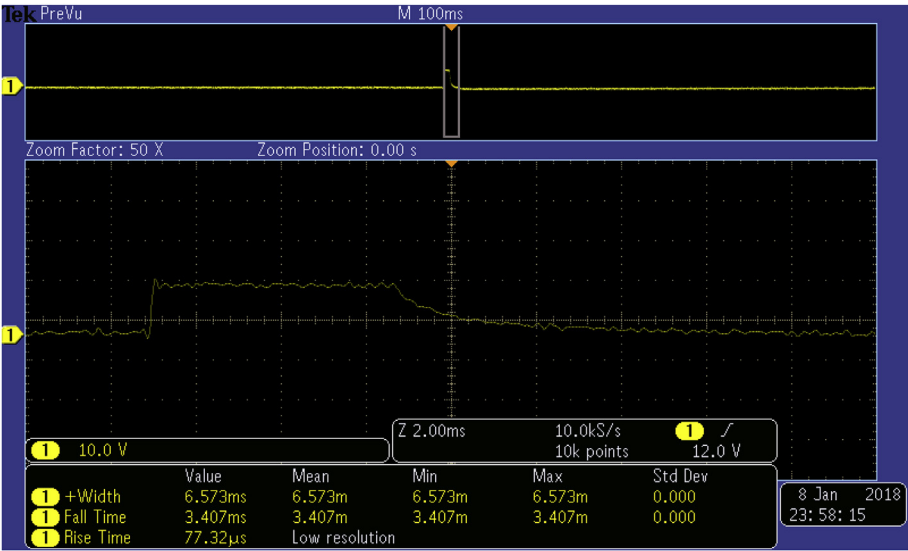


Fig. 3. A pulse from background radiation is shown on the oscilloscope's screen. There is only one pulse observed during the whole 100 ms duration.

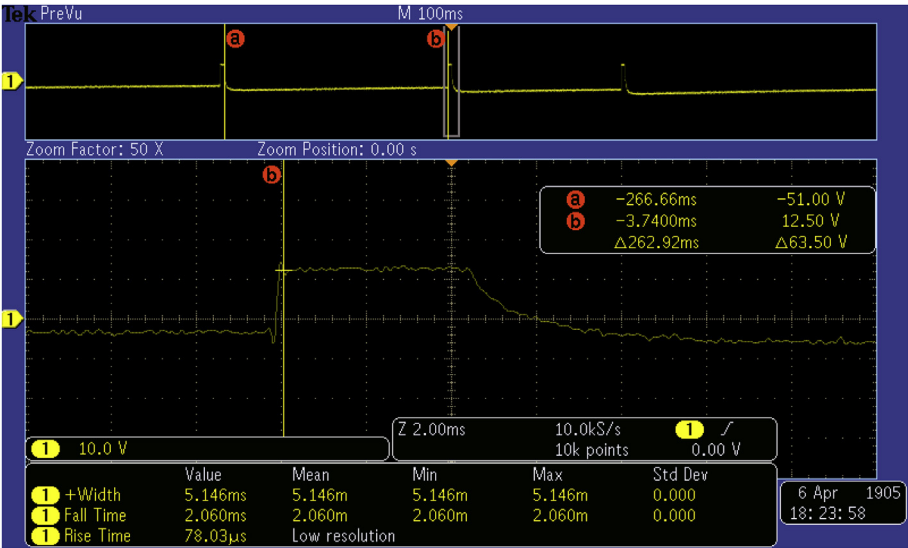


Fig. 4. A train of three pulses were captured in a 100 ms duration for <sup>60</sup>Co. Cursors a and b, on the top of the screen, show the measurement of lapse time between the first and second pulse. The lapse time is 262.92 ms. The second pulse on the bottom of the screen was zoomed to 2 ms for detailed analysis.

pulse shapes and pulse characteristics definitions observed during the experiments. Pulse characteristics were recorded using automatic measurement capabilities of the oscilloscope.

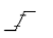


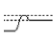





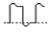
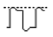

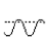
The experiment was conducted in three parts. In the first part, the GM counter was used to detect radiation incidents from background radiation. The voltage was set at 370 V because at that voltage the GM counter started to register the radiation incidents which were displayed simultaneously on the oscilloscope's screen. Subsequently, starting with 400 V, measurements were taken at various voltages with a 50 V increment until 1000 V. The pulse/s on the screen were captured using the oscilloscope's run/stop option for a duration of 100 ms. Each pulse shape characteristics was analyzed individually using the auto-measurement option. The data obtained from the pulse shape characteristics were entered manually in Microsoft Excel for further analysis; and the image of the observed pulse/s were saved to the PC, as shown in Fig. 3. For each of the tested voltage, 15 independent observations were made for pulse size and shape analysis.

The second part of the experiment followed the same procedure

with  $^{60}\text{Co}$  source. The source was placed on a transparent plastic tray 3 cm away from the GM counter. Unlike background radiation where only one pulse at a time was observed on the oscilloscope's screen due to the low number of radiation incidents, the  $^{60}\text{Co}$  source had ensued multiple pulses were simultaneously observed on the oscilloscope's screen, as illustrated in Fig. 4. To be consistent across all measurements of the second and third part of the experiment, we decided to capture a train of three pulses or more at a time on the oscilloscope screen to investigate the effect of pulse lapse time on the second pulse characteristics. In addition, the time between the onset of the first and second pulse was measured manually using the two cursors (a and b) knobs on the oscilloscope. The measurement started from the rising edge of the first pulse and ended at the rising edge of the second pulse. The time measured between the two pulses was defined as lapse time. The lapse time between the second and third pulse was also recorded. The train of three pulses that were captured was assigned as one trail. Again, a total of 15 trails were recorded for the  $^{60}\text{Co}$  source. In the third part, the same procedure was followed using  $^{137}\text{Cs}$  source.

**Table 1**

Each automatic measurement illustration of pulse definition. The rise and fall time along with the pulse width are time measurements while others are amplitude in the units of volts.

Illustration	Measurement	Definition
	Rise Time	It is the time required for the leading edge to rise from the low reference value (10%) to the high reference value (90%) of the final value.
	Fall Time	It is the time required for the falling edge to fall from the high reference value (90%) to the low reference value (10%) of the final value. The fall time is known as tail of the pulse.
	Pulse Width	It is the time between the mid reference (50%) amplitude point of the pulse.
	Positive Overshoot	Positive overshoot = (Max – High)/amplitude x 100%.
	Negative Overshoot	Negative overshoot = (Low – Min)/amplitude x 100%.
	Pk-Pk	It is the absolute difference between Max and Min amplitude of the pulse.
	Amplitude	It is the high value less the low value measured over the entire pulse.
	High	This value used as 100% whenever high reference, mid reference, or low reference values are needed of the entire pulse.
	Low	This value used as 0% whenever high reference, mid reference, or low reference values are needed of the entire pulse.
	Max	It is the most positive peak voltage over the entire pulse.
	Min	It is the most negative peak voltage over the entire pulse.
	RMS	The true Root Mean Square voltage over the entire pulse.
	Area	It is a voltage over time measurement where the area over the pulse is expressed in volt-seconds. The area above the baseline is positive and negative under the baseline.

**Table 2**

Background radiation and its pulse shape measurements using GM counter at different applied voltages.

Voltage (V)	Pulse Width (ms)	Fall Time (ms)	PK-PK (V)	Area (mVs)	Negative overshoot (%)
370	6.473	3.674	13.467	89.459	8.658
400	6.322	3.245	14.213	83.330	9.504
450	6.224	3.110	14.800	76.899	14.391
500	5.945	2.692	15.387	67.165	18.998
550	5.750	2.017	15.813	62.712	26.075
600	5.557	1.791	16.453	55.083	33.121
650	5.260	1.525	18.080	32.684	40.445
700	5.194	1.422	18.213	33.971	44.595
750	5.049	1.270	19.093	21.918	50.541
800	4.897	1.184	19.680	15.384	56.090
850	4.814	1.083	20.107	11.894	60.904
900	4.666	1.012	20.747	5.362	66.419
950	4.562	0.924	21.360	–3.411	67.621
1000	4.311	0.805	22.587	–23.056	71.857



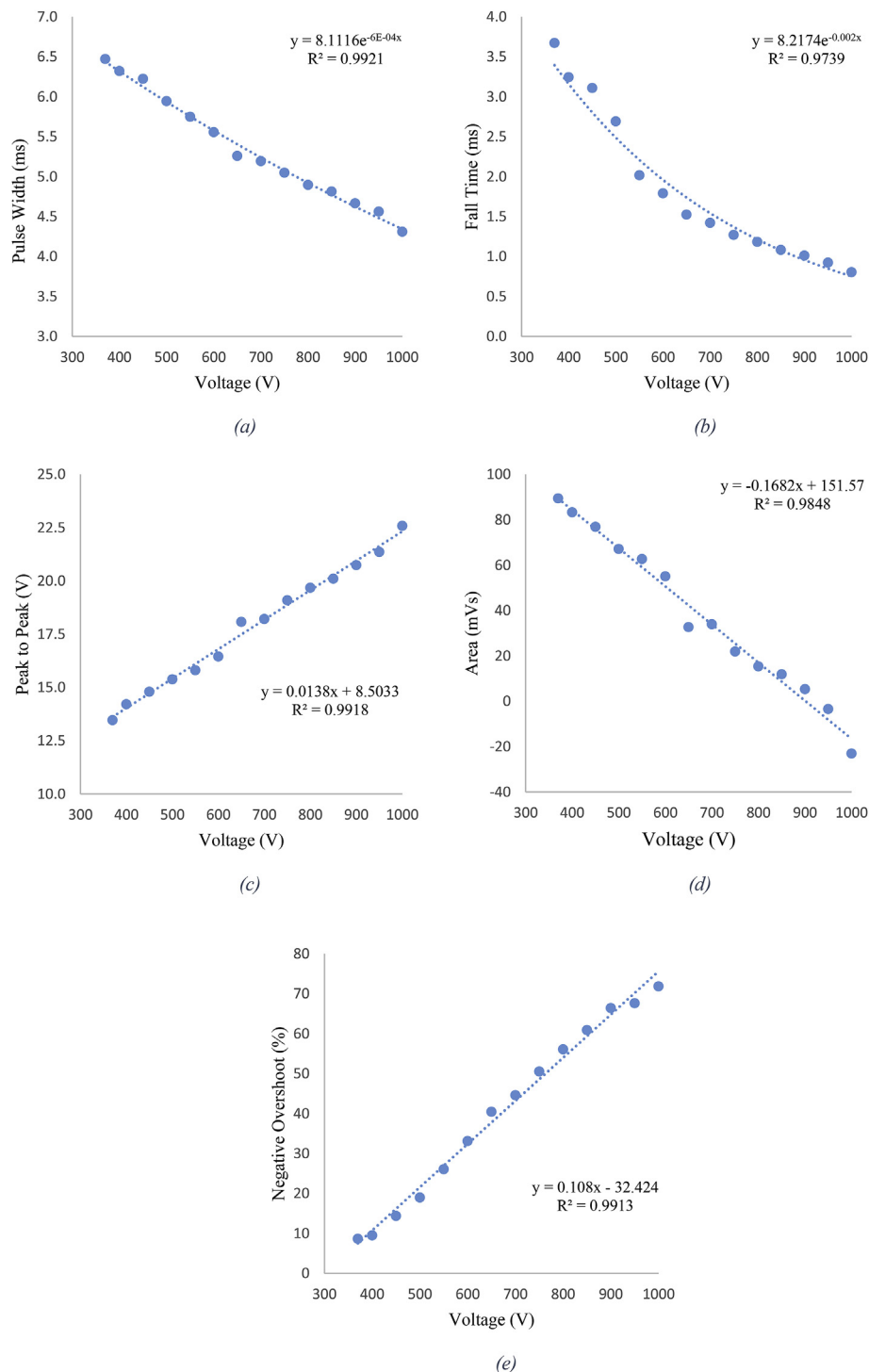
### 3. Results

All the pulses recorded were analyzed using the pulse characteristics described in Table 1. As an example, Table 2 shows pulse properties for 370 V and above while recording background radiation. No pulses were registered by the detection system below 370 V. Fall time (row 2, Table 1), pulse width (row 3, Table 1), peak to peak (row 6, Table 1), area (row 13, Table 1), and negative

overshoot (row 5, Table 1) for each pulse was recorded and averaged for the applied voltage for 15 independent measurements.

#### 3.1. Background radiation

First, pulses due to background radiation from the GM counter were captured and analyzed. Table 2 display the averages for the pulse properties as observed experimentally. Fig. 5(a) shows the



**Fig. 5.** Pulse shape measurements for background radiation using GM counter at different applied voltages: (a) pulse width measurements vs. voltage; (b) fall time vs. voltage; (c) Peak to Peak vs. voltage; (d) area of each recorded pulse vs. voltage; and (e) negative overshoot vs. voltage.

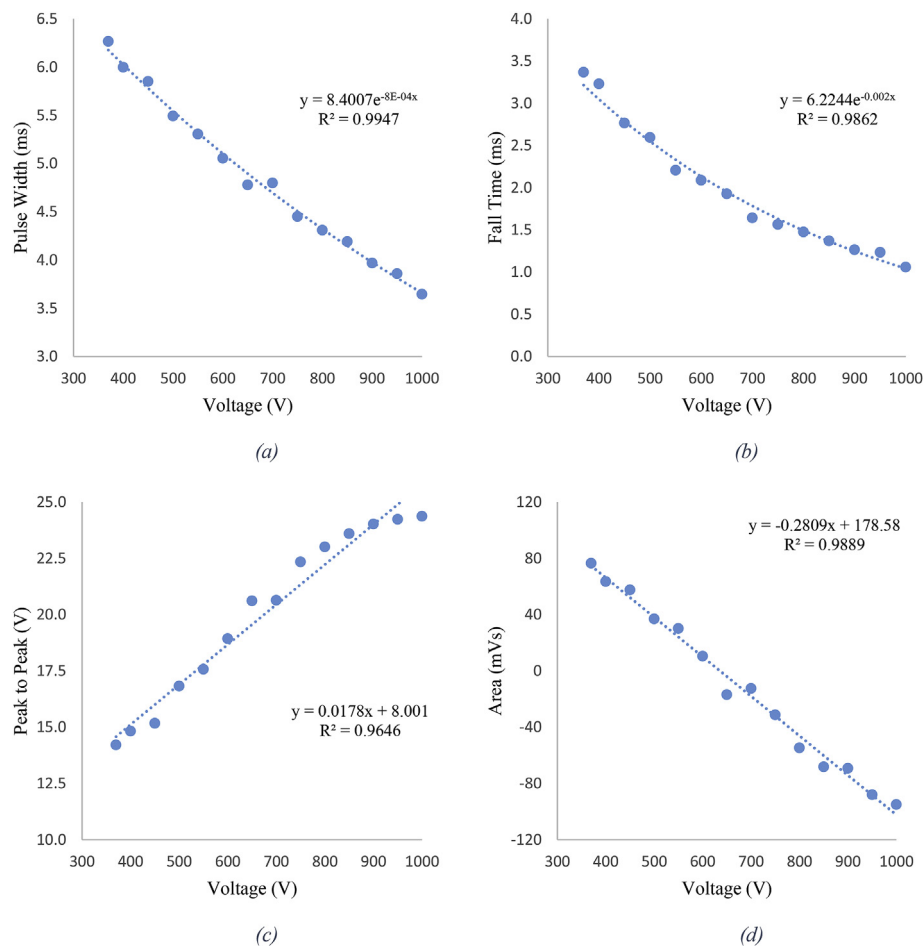
**Table 3**  
Pulse shape data for Co-60 source using GM counter at different applied voltages.

Voltage (V)	Pulse Width (ms)	Fall Time (ms)	PK-PK (V)	Area (mVs)
370	6.267	3.367	14.213	76.541
400	5.999	3.230	14.827	63.550
450	5.851	2.765	15.173	57.649
500	5.492	2.595	16.827	36.994
550	5.305	2.207	17.573	30.140
600	5.055	2.087	18.933	10.502
650	4.778	1.927	20.613	−16.890
700	4.798	1.642	20.640	−12.466
750	4.450	1.563	22.347	−31.318
800	4.309	1.473	23.013	−54.687
850	4.190	1.368	23.600	−68.173
900	3.969	1.263	24.027	−69.202
950	3.859	1.234	24.240	−87.987
1000	3.646	1.059	24.373	−94.982

pulse width dependence on the operating voltage, pulse width seems to drop exponentially with increasing voltage. While for this limited data set, linear fit was also good but the  $R^2$  value for the exponential fit was better. The exponential dependence of the pulse fall time (row 2) is apparent in Fig. 5(b) suggesting a reduced charge collection time at high operating voltage. Pulse height or peak-to-peak voltage as shown in Fig. 5(c) seems to have a linear relationship (for background data only, when there is no discrete gamma energy is involved) with the operating voltage with a  $R^2 = 0.99$ . As

seen in Fig. 5(d), pulse area (row 13, Table 1) for the low background count rate was mostly positive except for the two highest operating voltages. The relationship between the operating voltage and the pulse area seems to be linear with  $R^2 = 0.985$ . For low count rates, the negative overshoot was also observed to be linearly dependent on the operating voltage as can be seen in Fig. 5(e). After collecting the data on the background pulses, two sources,  $^{137}\text{Cs}$  and  $^{60}\text{Co}$  were introduced independently to investigate the effect of gamma energy on the pulse characteristics. Generally, it is believed that all pulses from a GM counter are identical in all their characteristics, independent of the radiation type and energy. We wanted to show some fine differences in the pulse characteristics depending on the initiating radiation energy.

Each average is taking over 15 independently observed pulses. The background pulses were captured because in the measurement of deadtime, background counts are also collected and subtracted from the final calculations. Due to the low intensity of background radiation in comparison with the  $^{137}\text{Cs}$  and  $^{60}\text{Co}$  sources, only negative overshoot showed a linear fit as can be seen in Fig. 5(e). Nevertheless, negative overshoot of the  $^{137}\text{Cs}$  and  $^{60}\text{Co}$  sources showed no relationship because of the high intensity of the sources that resulted in high count rates. Hence, negative overshoot data were not included in the analysis of  $^{137}\text{Cs}$  and  $^{60}\text{Co}$  pulse characteristics.



**Fig. 6.** Pulse shape measurements for Co-60 source using GM counter at different applied voltages: (a) pulse width measurements vs. voltage; (b) fall time vs. voltage; (c) Peak to Peak vs. voltage; and (d) area of each recorded pulse vs. voltage.

**Table 4**  
Pulse shape data for Cs-137 source using GM counter at different applied voltages.

Voltage (V)	Pulse Width (ms)	Fall Time (ms)	PK-PK (V)	Area (mVs)
370	6.328	3.328	13.920	81.557
400	6.125	3.273	14.693	68.735
450	5.818	3.220	16.107	49.635
500	5.693	2.650	16.533	47.731
550	5.407	2.134	17.387	36.883
600	5.040	2.068	19.200	3.707
650	4.920	1.795	20.187	-7.141
700	4.810	1.596	20.453	-18.212
750	4.466	1.518	22.347	-46.443
800	4.275	1.439	22.827	-53.130
850	4.219	1.387	23.387	-58.021
900	4.124	1.156	23.493	-61.792
950	4.082	1.177	23.520	-62.491
1000	3.981	1.038	23.547	-67.129

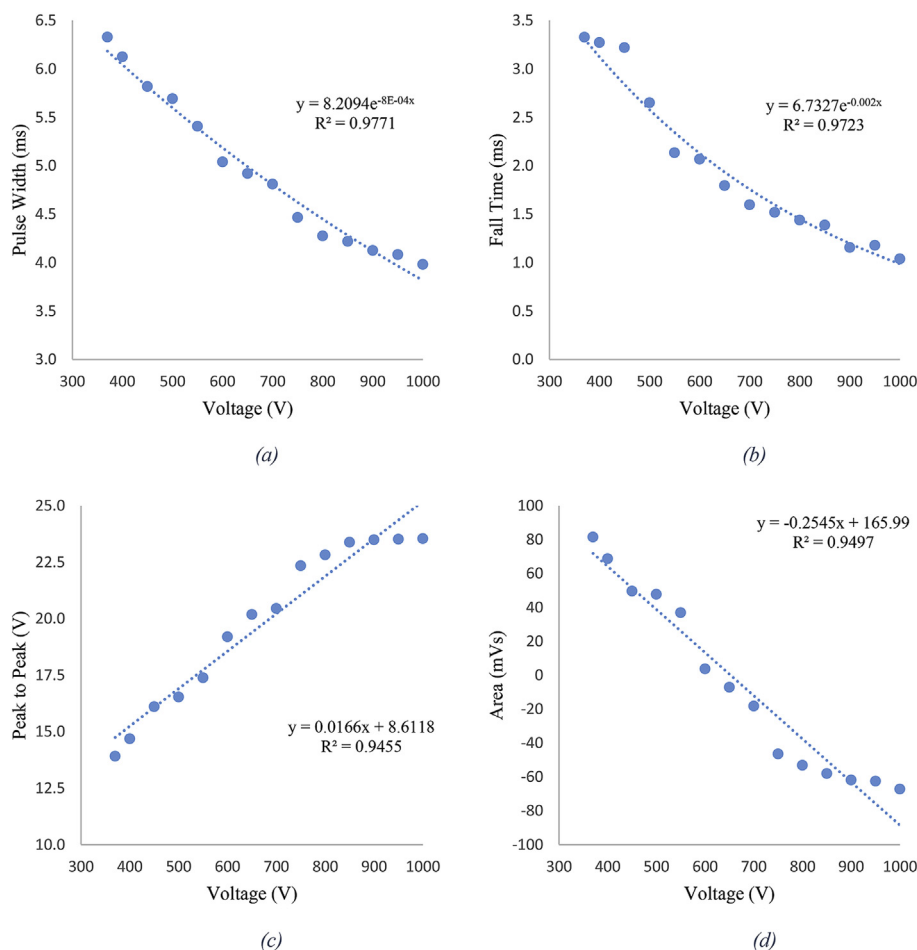
### 3.2. $^{60}\text{Co}$ source

Second,  $^{60}\text{Co}$  pulses from the GM counter were analyzed.  $^{60}\text{Co}$  decays with a half-life of 5.272 years emitting two discrete gammas; 1.1732 MeV (99.85%) and 1.3324 MeV (99.98%) [24]. Averages of pulse characteristics for 15 pulses observed with  $^{60}\text{Co}$  is shown in Table 3. Generally, data follows the similar behavior as the background except for peak to peak voltages. For  $^{60}\text{Co}$ , peak-to-peak data does seem to deviate from the linear fit, and it appears

to show an asymptotic peak-to-peak value for higher operating voltage as shown in Fig. 6(c). What it physically means is that, at high operating voltage a maximum peak-to-peak is reached and increasing operating voltage further will not impact the pulse peak-to-peak height. Data collection was restricted to 1000 V to avoid any permanent damage to the detector. The area under the curve also showed a linear dependence on the applied voltage. These results are quite revealing for the inside working of the GM counter and careful data analysis would help the radiation measurement community to gain insight on GM operation.

### 3.3. $^{137}\text{Cs}$ source

Lastly,  $^{137}\text{Cs}$  pulses from the GM counter were analyzed.  $^{137}\text{Cs}$  has a half-life of 30.08 years and it emits one discrete gamma at 0.661 MeV (85.1%) [25]. Pulse characteristics averaged for 15 pulses observed with  $^{37}\text{Cs}$  are shown in Table 4. Generally, data follows a similar behavior as  $^{60}\text{Co}$ . However, there are some subtle differences between the pulses from the two gamma sources. For example,  $^{60}\text{Co}$ , peak-to-peak data seem reach an asymptotic value which is higher than  $^{137}\text{Cs}$  asymptotic value. The other significant difference was the poor linear relationship between the pulse area and the operating voltage. As seen in Fig. 7(d), the linear fit is perhaps not the best description of the data. These fine differences will be discussed in the conclusion section of the manuscript.



**Fig. 7.** Pulse shape measurements for Cs-137 source using GM counter at different applied voltages: (a) pulse width measurements vs. voltage; (b) fall time vs. voltage; (c) Peak to Peak vs. voltage; and (d) area of each recorded pulse vs. voltage.



#### 4. Conclusion & discussion

Based on the data collected, the general belief that all pulses from a GM counter from any intensity, type and/or energy of radiation source are identical is questionable. While the pulse shape does not carry any important information for simple count rate application, it does have an impact on the detector deadtime behavior. When comparing the peak-to-peak pulse height, it is evident that both  $^{60}\text{Co}$  and  $^{137}\text{Cs}$  have an asymptote as shown in Fig. 8. It is difficult to draw any definite conclusion about the energy dependence of the asymptote with only two radiation sources. However, one is compelled to notice that  $^{60}\text{Co}$  (with higher gamma energy) has asymptote which is higher than that of  $^{137}\text{Cs}$  (with lower gamma energy). If more data becomes available with a wide spectrum of gamma energies, one would be able to develop a relationship between the asymptote peak-to-peak voltage and gamma energy.

Similarly, one is bound to notice that the exponent for the pulse fall time ( $-0.002$ ) is independent of the source of radiation. For all three cases; background,  $^{60}\text{Co}$  and  $^{137}\text{Cs}$  the pulse fall time dependence on voltage remains unchanged. The other interesting observation is the slower/weaker voltage dependence of the pulse width as compared to the pulse fall time. The exponent for pulse width was found to be  $-6.0\text{E-}4$  for the background measurement while it is  $-8.0\text{E-}4$  for both  $^{60}\text{Co}$  and  $^{137}\text{Cs}$  which is much smaller than  $-2.0\text{E-}3$  for the pulse fall time. What it means is that the main body of the pulse is weakly dependent on the applied voltage than the pulse tail.

Furthermore, detector deadtime was earlier reported to depend on applied voltage [3]. As discussed earlier [3], there are three distinct region of detector deadtime. At lower voltages, the deadtime reduced with increasing voltage. In this region, as the data presented here suggests, the pulse duration (pulse width plus fall time) is also decreasing with increasing voltage. Consequently, the

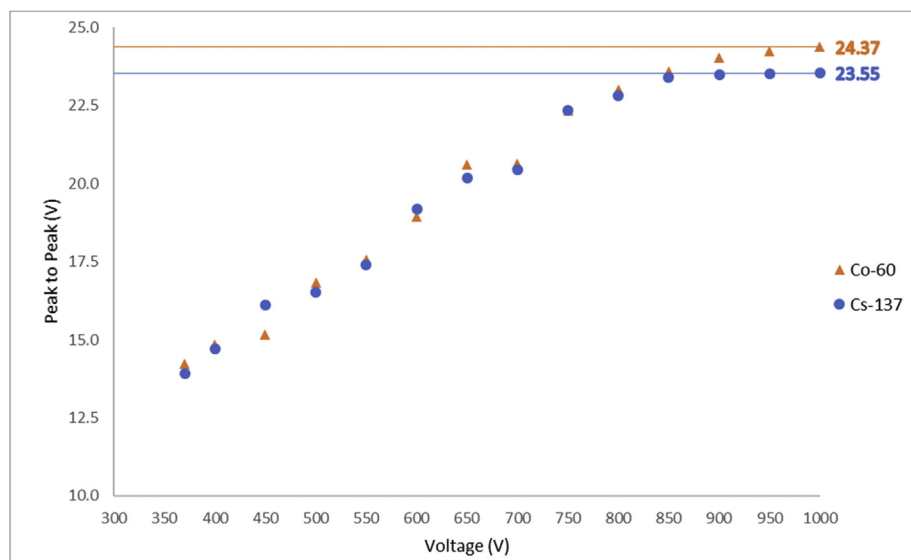


Fig. 8. Comparison of Peak to Peak dependence of voltage for  $^{60}\text{Co}$  and  $^{137}\text{Cs}$ .

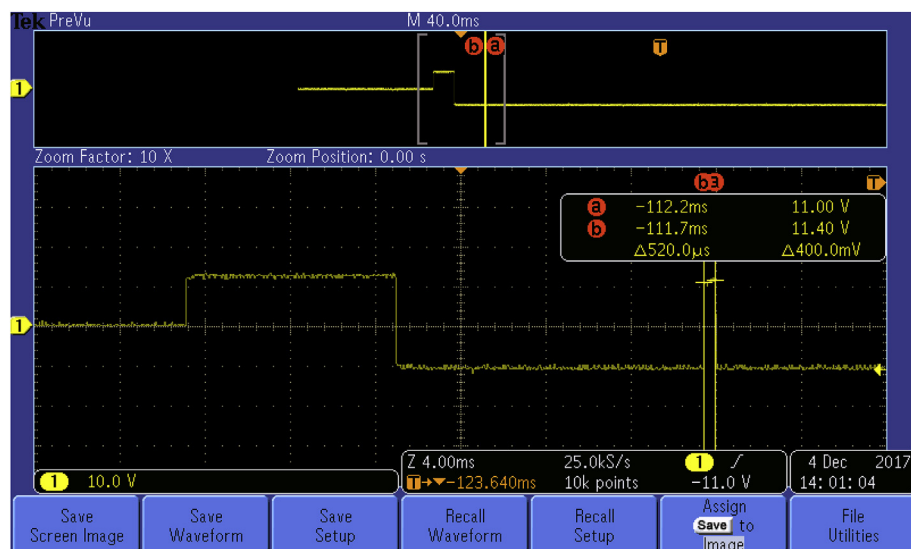


Fig. 9. Second pulse width reductions.

deadtime decreases with reducing pulse duration. This is because there is a lower probability of overlapping pulses with reduced pulse duration. The next region is the region of minimum constant deadtime. During this region, pulse tail has completely vanished, and the pulse width was observed to be its minimum. The lower end of this plateau region is best for GM counter operations. Increasing the voltage further will result in second pulse (after an initial pulse) width reduction. The second pulse duration reduction depends not only on the applied voltage but also on the time lapse between the two pulses. Fig. 9 shows the screenshot of the reduced second pulse width, 520  $\mu$ s. Based on the new data presented here there is a strong possibility that one could develop a pulse shape correlation for the detector deadtime.

## Nomenclature

GM	Geiger-Mueller
$v$	Drift Velocity
$\mu$	Mobility
$E$	Strength of Electric Field
$p$	Pressure
$m$	Observed or Measured Count Rate
$n$	True Count Rate
$\tau$	Deadtime
$\tau_p$	Paralyzing Deadtime
$\tau_{np}$	Non-Paralyzing Deadtime
$f$	Paralysis Factor

## Appendix A. Supplementary data

Supplementary data to this article can be found online at <https://doi.org/10.1016/j.net.2019.02.008>.

## References

- [1] H. Geiger, W. Müller, Electron counting tube for the measurement of the weakest radioactivities, *Sciences* 16 (1928) 617–618.
- [2] G.F. Knoll, *Radiation Detection and Measurement*, third ed., John Wiley & Sons Inc., USA, 2000.
- [3] T. Akyurek, M. Yousaf, X. Liu, S. Usman, GM counter deadtime dependence on

- applied voltage, operating temperature and fatigue, *Prog. Nucl. Energy* 73 (2015) 26–35.
- [4] J.C. May, D.H.J. Russell, A mass-selective variable-temperature drift tube ion mobility-mass spectrometer for temperature dependent ion mobility studies, *J. Am. Soc. Mass Spectrom.* 22 (2011) 1134–1145.
- [5] H.G. Stever, The discharge mechanism of fast G–M counters from the dead-time experiment, *Phys. Rev.* 61 (1942) 38–52.
- [6] J.W. Müller, Dead-time problems, *Nucl. Instrum. Methods* 112 (1973) 47–57.
- [7] S.M. Skinner, The efficiency of the tube counter, *Phys. Rev.* 48 (1935) 438–447.
- [8] L. Costrell, Accurate determination of the deadtime and recovery characteristics of Geiger-Muller counters, *J. Res. Natl. Bur. Stand.* 42 (3) (1949) 241–249.
- [9] J.H. Lee, I.J. Kim, H.D. Choi, On the dead time problem of a GM counter, *Appl. Radiat. Isot.* 67 (6) (2009) 1094–1098.
- [10] R.P. Gardner, L. Liu, On extending the accurate and useful counting rate range of GM counter detector system, *Appl. Radiat. Isot.* 48 (1997) 1605–1615.
- [11] S.H. Lee, R.P. Gardner, A new G–M counter dead time model, *Appl. Radiat. Isot.* 53 (2000) 731.
- [12] A. Patil, S. Usman, Measurement and application of paralysis factor for improved detector dead time characterization, *Nucl. Technol.* 165 (2) (2009) 249–256.
- [13] T. Akyurek, L.P. Tucker, X. Liu, S. Usman, Portable spectroscopic fast neutron probe and  $^3\text{He}$  detector dead-time measurements, *Prog. Nucl. Energy* 92 (2016) 15–21.
- [14] M. Yousaf, T. Akyurek, S. Usman, A comparison of traditional and hybrid radiation detector dead-time models and detector behavior, *Prog. Nucl. Energy* 83 (2015) 177–185.
- [15] N. Tsoulfanidis, S. Landsberger, *Measurement and Detection of Radiation*, third ed., CRC Press, New York, 2012.
- [16] W. Feller, On probability problems in the theory of counters, in: *R. Courant Anniversary Volume, Studies and Essays*, Interscience, New York, 1948, pp. 105–115.
- [17] R.D. Evans, *The Atomic Nucleus*, McGraw-Hill, New York, 1955.
- [18] S. Usman, B. Almutairi, T. Akyurek, A new phenomenological model for Geiger-Müller deadtime, *Trans. Am. Nucl. Soc.* 117 (2017) 496–498.
- [19] Cesium-137 Source, <http://www.spectrumtechniques.com/wp-content/uploads/2016/12/Cesium-137-Information-Sheet.pdf>.
- [20] G-M counter, <https://ludlums.com/products/all-products/product/model-133-2>.
- [21] Ortec 142A/B/C Preamplifiers, <https://www.ortec-online.com/-/media/ametektortec/brochures/142abc.pdf>.
- [22] Ortec High-Voltage Power Supply, <https://www.ortec-online.com/-/media/ametektortec/brochures/556-556h.pdf>.
- [23] Tektronix Digital Phosphor Oscilloscopes, <https://www.tek.com/bench-oscilloscopes/mso3000-dpo3000-manual/mso3000-and-dpo3000-series>.
- [24] E. Browne, J. K Tuli, Table of nuclides for Co-60, ENSDF, international atomic energy agency, *Nucl. Data Sheets* 114 (2013) 1849.
- [25] E. Browne, J. K Tuli, Table of nuclides for Cs-137, ENSDF, international atomic energy agency, *Nucl. Data Sheets* 108 (2007) 2173.